LOW AND HIGH FIELD SCALING LIMITS FOR THE VLASOV- AND WIGNER-POISSON-FOKKER-PLANCK SYSTEMS

A. Arnold[1], J. A. Carrillo*[2], I. Gamba[2], C.-W. Shu[3]

July 24, 1999

[1]Fachbereich Mathematik, TU-Berlin, MA 6-2,

Straße des 17. Juni 136, D-10623 Berlin, Germany

[2]Department of Mathematics,

University of Texas at Austin, Austin, TX 78712.

[3]Division of Applied Mathematics,

Brown University, Providence, RI 02912

Abstract

This paper is concerned with scaling limits in kinetic semiconductor models. For the classical Vlasov-Poisson-Fokker-Planck equation and its quantum mechanical counterpart, the Wigner-Poisson-Fokker-Planck equation, three distinguished scaling regimes are presented. Using Hilbert and Chapman-Enskog expansions, we derive two drift-diffusion type approximations. The test case of a $n^+ - n - n^+$ diode reveals that different scaling regimes may be present at the same time in different subregions of a semiconductor device. Numerical simulations of the stationary solution illustrate the good approximation of the kinetic solution by a drift-diffusion model and by a hybrid (adaptive domain decomposition) model.

AMS 1991 Subject Classification: 35B25, 76P05, 82C70, 65M99

Key words: Semiconductor models, Vlasov-Poisson-Fokker-Planck equation, drift-diffusion models, scaling limits, domain decomposition

1 Introduction

As a basic model for the electron transport in a semiconductor device one can consider the semiclassical Boltzmann equation which, in the parabolic band approximation, can be written as (see [20])

$$\frac{\partial f}{\partial t} + (v \cdot \nabla_x) f - \frac{e}{m}(E(t,x) \cdot \nabla_v) f = \mathcal{Q}(f,f). \tag{1.1}$$

$f = f(t,x,v)$ is the phase space density function for an electron of position $x \in \Omega \subset I\!R^N$ and velocity $v \in I\!R^N$ at time $t \geq 0$, where Ω is the domain of the device. The constants e and m represent the unit charge and effective electron mass, respectively.

The electric field $E = E(t,x)$ is self-consistently produced by the electrons moving in a fixed ion background with density $C(x)$. E is determined by the Poisson equation

$$\begin{aligned} \mathrm{div}_x(\varepsilon(x)\nabla\Phi) &= e(\rho(f) - C(x)), \\ E(t,x) &= -\nabla\Phi, \end{aligned} \tag{1.2}$$

where ε is the permittivity of the material and

$$\rho(f)(t,x) = \int_{I\!R^N} f(t,x,v)dv, \quad j(f)(t,x) = \int_{I\!R^N} vf(t,x,v)dv, \quad x \in \Omega,\ t \geq 0 \tag{1.3}$$

are, respectively, the charge and current densities of the electrons.

The form of the collision operator $\mathcal{Q}(f,f)$ can take into consideration different interactions: electrons with background impurities, phonon-electron collisions, electron-electron short range interactions and so on. We refer to [26] for a complete list of scattering kernels.

In the low density approximation and taking into account only collisions with background impurities, one can approximate $\mathcal{Q}(f)$ by a linear relaxation time operator [10, 11, 14, 20] given by

$$\mathcal{Q}(f) = \frac{1}{\tau}(M_\Theta \rho(f) - f), \tag{1.4}$$

where $\tau = \tau(x)$ or $\tau = \tau(E(t,x))$, constant in v, is an approximation for the relaxation time $\tau(x,v)$. M_Θ is the absolute Maxwellian at the temperature of the semiconductor given by

$$M_\Theta = (2\pi\Theta)^{-N/2} \exp\left(-\frac{|v|^2}{2\Theta}\right),$$

where $\Theta = \Theta(x)$ is the lattice temperature ($\Theta = k_B \frac{T}{m}$ with the Boltzmann constant k_B, and T is the lattice temperature in Kelvin). A drift-collision balance scaling for the system (1.1)-(1.2) with Q given by (1.4) was studied in [10, 11].

In this paper we are going to consider another possibility to model the lattice collision operator $\mathcal{Q}(f)$. The hydrodynamical semiconductor models describe the

motion of the electrons as a fluid, while kinetic Boltzmann–type semiconductor equations treat the scattering process in a very detailed way by looking at the electrons as individual particles. There is a middle ground in this description (mesoscopic model [31]); this is offered by the Brownian dynamics in which we consider the paths of individual electrons but we take into account the scattering processes in average. This modeling of the scattering is useful in some cases, e.g. to study noise in semiconductor devices (see [14] chapter 4 and 10, [19] chapters 1-3 and [31]).

Assuming that the interaction of the electrons with the lattice introduces a Brownian motion on the electrons, the electrons follow the paths of the stochastic differential equation

$$x'' + \frac{1}{\tau(x)}x' - \frac{e}{m}E(t,x) = \Gamma(t).$$

Here, $\tau(x)$ (or $\tau = \tau(E(t,x))$) is the relaxation time and $\Gamma(t)$ is a white noise stochastic force produced by the interaction with the lattice with independent, identically Gaussian distributed processes of variance $\frac{\Theta(x)}{\tau(x)}$.

Applying Ito's equation for the probability density corresponding to the solution of the above stochastic Langevin equation (Newton's law), the collision operator is given by the so-called Fokker-Planck (FP) operator

$$\mathcal{Q}_1(f) = L_{FP}f = \frac{1}{\tau}\mathrm{div}_v(vf + \Theta\nabla_v f). \tag{1.5}$$

The full transient kinetic equation is then given by

$$\frac{\partial f}{\partial t} + (v\cdot\nabla_x)f - \frac{e}{m}(E(t,x)\cdot\nabla_v)f = \frac{1}{\tau}\mathrm{div}_v(vf + \Theta\nabla_v f), \tag{1.6}$$

coupled to the Poisson equation (1.2). The system of equations (1.6)-(1.2) is called the Vlasov-Poisson-Fokker-Planck (VPFP) system. Both the relaxation time operator (1.4) and the FP operator drive the system towards the equilibrium density given by M_Θ with rate τ. Hence, both are candidates for simple models of the lattice collision operator $\mathcal{Q}(f)$ and both are used in applications ([14], [31]).

The quantum-mechanical analogue of (1.6)-(1.2) is called the Wigner-Poisson-Fokker-Planck equation (WPFP). The WPFP equation models the self-consistent transport of an electron ensemble in quantum semiconductor devices (see [30, 16]), and it reads ([1, 6, 13])

$$\frac{\partial w}{\partial t} + (v\cdot\nabla_x)w - \frac{e}{m}T_{\hbar/m}[\Phi]w = \frac{1}{\tau}L_{QFP}w, \tag{1.7}$$

coupled to the Poisson equation (1.2). Here, $w(t,x,v)$ is the (real-valued, but *not* pointwise non-negative) Wigner distribution function (see [32, 20] for a detailed discussion of its properties). As in the above classical case, the charge and current densities are respectively given by

$$\rho(w)(t,x) = \int_{\mathbb{R}^N} w(t,x,v)dv, \quad j(w)(t,x) = \int_{\mathbb{R}^N} vw(t,x,v)dv, \quad x\in\Omega,\ t\geq 0. \tag{1.8}$$

While $w(t,x,v)$ may take negative values, $\rho(w)(t,x) \geq 0$ for "physical" Wigner functions (see [1, 20] for details).

The electrostatic potential $\Phi(t,x)$ enters in (1.7) via the pseudo-differential operator

$$(T_{\hbar/m}[\Phi]w)(t,x,v) \tag{1.9}$$
$$= \tfrac{i}{(2\pi)^N} \int_{I\!R^N_\xi} \int_{I\!R^N_{v'}} \tfrac{\Phi(t,x+\frac{\hbar}{2m}\xi)-\Phi(t,x-\frac{\hbar}{2m}\xi)}{\hbar/m} w(t,x,v') \exp(-i(v-v')\cdot\xi)\, dv'\, d\xi,$$

with $\hbar$ denoting the Planck constant. In the classical limit ($\hbar \to 0$) $T_\hbar[\Phi]w$ formally yields its classical counterpart from (1.6), i.e. $-\nabla_x\Phi\cdot\nabla_v w$. Due to the non-locality of (1.9), the potential Φ has to be known on the whole space $I\!R^N_x$. If the WPFP equation is considered on a bounded domain Ω, Φ has therefore to be appropriately continued outside of Ω (see [18] for possible extension strategies in 1D).

In (1.7) the quantum Fokker-Planck term on the R.H.S. models the interaction of the electrons with the phonons of the crystal lattice, and it reads:

$$L_{QFP}w = \mathrm{div}_v(vw + \Theta\nabla_v w) + \frac{\omega_P\hbar^2}{6\pi m^2\Theta}\mathrm{div}_x(\nabla_v w) + \frac{\hbar^2}{12m^2\Theta}\Delta_x w, \tag{1.10}$$

where ω_P denotes the cut-off frequency of the crystal phonons (see [1, 13]). In the classical limit the last two terms of (1.10) disappear such that one then recovers the VPFP system. In contrast to the classical situation, the relaxation time τ and the lattice temperature Θ have to be constant (in x) for the WPFP model; otherwise the model would not be quantum-mechanically correct (see [1]).

In this paper we present different scalings and their macroscopic scaling limits for both systems (VPFP and WPFP) corresponding to low and high local field effects (Section 2). In the case of high local fields we consider two different scalings depending on the balance between collisions and the electric field: drift-collision balance scaling and ballistic scaling. Also, we compute the scaling limit for the low field scaling for both systems leading to drift-diffusion type equations coupled to the Poisson equation. In the quantum case we will find quantum corrections to the corresponding classical equations (Section 3). In the drift-collision balance scaling (Section 4) we use a Chapman–Enskog type expansion to calculate corrections to the drift-diffusion equation that are of higher order in the expansion parameter. In the quantum case we shall again compute its quantum corrections. We will discuss the differences with the results obtained in [11] for the relaxation time operator (1.4). In Section 5 we discuss the ballistic scaling and revisit the drift-collision balance scaling. Also, we discuss the conditions under which these two different high-field scalings can be applied. Finally, the last section is devoted to the numerical approximation of the VPFP system for a one dimensional silicon device for which we show that all three scaling regimes are relevant in different situations. For this test case we shall compare the solution of the kinetic VPFP equation to the solution of its drift-diffusion type approximations, which are computationally much cheaper to obtain.

The scalings leading to low field equations and drift-collision balance equations for a linear Boltzmann equation of the type (1.4) with a known external potential

were introduced in the mathematical literature in [23, 24, 29]. The ballistic regime has been used for the relaxation time operator in [3]. The correction terms for the self-consistent case were computed in the case of the relaxation operator (1.4) in [10, 11] and very preliminary numerical device simulations have been presented in [8] and [9]. Our work follows this line of investigation. For a more complete account on the literature related to this problem we refer to [11].

2 Scaling and low/high field regimes

In this section we present the three scalings of the VPFP and the WPFP systems. Since the VPFP equation is obtained from the WPFP system by formally setting $\hbar = 0$, we will first scale the WPFP equation. For this calculation we will slightly generalize (1.7), (1.2) by admitting the relaxation time and the temperature to be x-dependent: $\tau = \tau(x)$, $\Theta = \Theta(x)$. The scaled VPFP and WPFP equations are then recovered as special cases.

Let L be the characteristic length of the device, ρ_0 the average value of the doping profile $C(x)$, and ε_0 a typical magnitude of the permittivity $\varepsilon(x)$.

Our evolution system incorporates four different time scales or, equivalently, characteristic velocities: With Θ_0 a typical value of the lattice temperature, $\Theta_0^{1/2}$ is the reference magnitude for the *thermal velocity.*

τ is called the *relaxation time* because, in the absence of forces and in the space-homogeneous FP equation,

$$\frac{\partial w}{\partial t} = \frac{1}{\tau_0}\mathrm{div}_v(vw + \Theta_0 \nabla_v w),$$

$w(t, v)$ relaxes to the Maxwellian equilibrium

$$M_{\Theta_0}(v) = (2\pi\Theta_0)^{-N/2} \exp\left\{-\frac{|v|^2}{2\Theta_0}\right\}$$

with a rate $\exp(-t/\tau_0)$ in the L^1-norm (see [7]). With τ_0 we denote a reference value for $\tau(x)$.

Let $[\Phi]$ be the potential drop ("bias") applied to the contacts of the device of length L. Then the reference magnitude for the *drift velocity* $U = -\tau\frac{e}{m}E$ is given by

$$U_0 = \tau_0 \frac{e}{m} E_0 = \tau_0 \frac{e}{m} \frac{[\Phi]}{L},$$

and the reference value for the *ballistic velocity* is

$$B_0 = \sqrt{2\frac{e}{m}[\Phi]}.$$

The name of ballistic velocity comes from the fact that for high fields we can assume that the collisions are negligible, and then the evolution of the system is given by

the Vlasov-Poisson system. Thus, the particles follow the paths of the underlying ordinary differential system conserving energy, that is,

$$m\frac{|v|^2}{2} - e\Phi(t,x) = const. \tag{2.1}$$

Let us obtain first the scaled equations for the first two scalings, namely, the low field scaling and the drift-collision balance scaling. With the above characteristic values we introduce new, non-dimensional variables as:

$$\begin{aligned} x = L\hat{x}, \qquad v = \Theta_0^{1/2}\hat{v}, \qquad t = \frac{L}{U_0}\hat{t}, \\ \tau(x) = \tau_0\hat{\tau}(\hat{x}), \quad \varepsilon(x) = \varepsilon_0\hat{\varepsilon}(\hat{x}), \quad C(x) = \rho_0\hat{C}(\hat{x}), \\ \Phi(t,x) = [\Phi]\hat{\Phi}(\hat{t},\hat{x}), \quad \Theta(x) = \Theta_0\hat{\Theta}(\hat{x}), \end{aligned} \tag{2.2}$$

and the scaled Planck constant is

$$h_0 = \frac{\hbar}{\tau_0 m \Theta_0}.$$

For the dimensionless Wigner distribution function $\hat{w}(\hat{t},\hat{x},\hat{v})$ we shall consider two possible choices of the density scale:

a)

$$w(t,x,v) = \frac{\rho_0}{\Theta_0^{N/2}}\hat{w}(\hat{t},\hat{x},\hat{v}), \tag{2.3}$$

or

b)

$$w(t,x,v) = \frac{\rho_0}{U_0^N}\hat{w}(\hat{t},\hat{x},\hat{v}). \tag{2.4}$$

When applying the above scaling with (2.3) to (1.7), (1.2) a straightforward calculation gives:

$$\begin{aligned} &\eta\frac{\partial w}{\partial t} + (v\cdot\nabla_x)w - \frac{\eta}{\nu}T_{\nu h_0}[\Phi]w \\ &= \tfrac{1}{\nu}\tfrac{1}{\tau(x)}\mathrm{div}_v(vw + \Theta(x)\nabla_v w) + \tfrac{\zeta h_0}{6\pi}\tfrac{1}{\tau(x)\Theta(x)}\mathrm{div}_x(\nabla_v w) + \tfrac{h_0^2\nu}{12}\tfrac{1}{\tau(x)\Theta(x)}\Delta_x w, \end{aligned} \tag{2.5}$$

and

$$\mathrm{div}_x(\varepsilon(x)\nabla_x\Phi) = \gamma(\rho(w) - C(x)) \tag{2.6}$$

(here and in the sequel we omit the "hat" on the new variables). Here, we introduced the following dimensionless parameters:

$$\eta = \frac{U_0}{\Theta_0^{1/2}}, \quad \nu = \frac{\tau_0\Theta_0^{1/2}}{L},$$

$$\gamma = \frac{\rho_0 e L^2}{\varepsilon_0[\Phi]}, \quad \zeta = \frac{\omega_P\hbar}{m\Theta_0}.$$

For the *low field scaling* (LFS) we assume first that $\eta \simeq \nu \ll 1$. This means that the drift velocity is small compared to the thermal velocity. This is precisely the reason we call this scaling "low field". And in turns, the thermal velocity is small compared to the "relaxation velocity" $\frac{L}{\tau_0}$, with both ratios being of the same order of magnitude.

We consider first the LFS of the (classical) VPFP equation, i.e. we set $h_0 = 0$ in (2.5):

$$\eta\frac{\partial f}{\partial t} + (v\cdot\nabla_x)f + (\nabla_x\Phi\cdot\nabla_v)f = \frac{1}{\eta}\frac{1}{\tau(x)}\mathrm{div}_v(vf + \Theta(x)\nabla_v f), \tag{2.7}$$

$$\mathrm{div}_x(\varepsilon(x)\nabla_x\Phi) = \gamma(\rho(f) - C(x)), \tag{2.8}$$

with $\eta \to 0$.

In the case of the WPFP system under the LFS regime, we recall from [1] the assumptions on the size of the parameters of L_{QFP} such that the QFP approximation is a reasonable model for electron-phonon interactions:

i) the memory time of the phonon reservoir is much smaller than the characteristic drift time of electrons: $\frac{1}{\omega_P} \ll \frac{L}{U_0}$,

ii) weak interaction between electrons and phonons: $\frac{1}{2\tau_0} \ll \omega_P$,

iii) medium to high temperatures: $\omega_P \lesssim \frac{m\Theta}{\hbar}$.

From the assumptions (ii) and (iii) we conclude

$$\zeta \lesssim 1, \qquad h_0 \ll 2. \tag{2.9}$$

In the quantum case we have to require $\tau = \tau_0,\ \Theta = \Theta_0$, and hence $\hat{\tau} \equiv 1,\ \hat{\Theta} \equiv 1$ follows from (2.2). Thus we obtain from (2.5), (2.6) the *LFS equations for the WPFP* system:

$$\eta\frac{\partial w}{\partial t} + (v\cdot\nabla_x)w - T_{\eta h_0}[\Phi]w = \frac{1}{\eta}\mathrm{div}_v(vw + \nabla_v w) + \frac{\zeta h_0}{6\pi}\mathrm{div}_x(\nabla_v w) + \frac{h_0^2\eta}{12}\Delta_x w, \tag{2.10}$$

together with (2.8) for $\eta \to 0$.

For the *drift-collision balance scaling* (DCBS) we use (2.2) and (2.4) to scale the VPFP and WPFP systems. We also assume that $\eta = O(1)$ and $\nu \ll 1$, which means that the drift and the thermal velocities are of comparable magnitude, but both are small compared to the relaxation velocity. Since the local values of the electric field are rather high in typical situations of this scaling (drift velocity $\simeq$ thermal velocity), we call it a "high field scaling." Setting, resp., $h_0 = 0$ and $\tau = 1$, $\Theta = 1$ in (2.5) we obtain the *DCBS equation for VPFP*:

$$\eta\frac{\partial f}{\partial t} + (v\cdot\nabla_x)f + \frac{\eta}{\nu}(\nabla_x\Phi\cdot\nabla_v)f = \frac{1}{\nu}\frac{1}{\tau(x)}\mathrm{div}_v(vf + \Theta(x)\nabla_v f), \tag{2.11}$$

and the *DCBS equation for WPFP*:

$$\begin{aligned}\eta\frac{\partial w}{\partial t} + (v\cdot\nabla_x)w - \frac{\eta}{\nu}T_{\nu h_0}[\Phi]w \\ = \frac{1}{\nu}\mathrm{div}_v(vw + \nabla_v w) + \frac{\zeta h_0}{6\pi}\mathrm{div}_x(\nabla_v w) + \frac{h_0^2\nu}{12}\Delta_x w,\end{aligned} \tag{2.12}$$

for $\nu \to 0$. Both (2.11) and (2.12) are coupled to the scaled Poisson equation

$$\mathrm{div}_x(\varepsilon(x)\nabla_x\Phi) = \gamma(\eta^{-N}\rho - C(x)), \tag{2.13}$$

with the charge density $\rho = \rho(f)$ or $\rho = \rho(w)$, resp.

Note that in both scalings of the WPFP system, (2.10) and (2.12), the quantum effects due to the operator $T_{\nu h_0}[\Phi]$ are rather small since $\nu h_0 \ll 1$.

Finally, let us obtain the *ballistic scaling* (BS) equations. To this end we have to choose different non-dimensional variables. We now set

$$v = B_0\hat{v}, \quad t = \frac{L}{B_0}\hat{t},$$

and the other variables are scaled like in (2.2). Hence the scaled Planck constant is

$$h_0^b = \frac{\hbar}{\tau_0 m B_0^2},$$

and the dimensionless Wigner distribution function $\hat{w}(\hat{t},\hat{x},\hat{v})$ is

$$w(t,x,v) = \frac{\rho_0}{B_0^N}\hat{w}(\hat{t},\hat{x},\hat{v}).$$

Introducing the dimensionless parameters

$$\alpha := \frac{U_0}{B_0} = \frac{\tau_0 B_0}{2L}, \quad \beta := \frac{\Theta_0^{1/2}}{B_0}, \tag{2.14}$$

the scaled equations read

$$\frac{\partial w}{\partial t} + (v\cdot\nabla_x)w - \frac{1}{2}T_{2\alpha h_0^b}[\Phi]w \tag{2.15}$$

$$= \frac{1}{2\alpha}\frac{1}{\tau(x)}\mathrm{div}_v(vw+\beta^2\Theta(x)\nabla_v w) + \frac{\zeta h_0^b}{6\pi}\frac{1}{\tau(x)\Theta(x)}\mathrm{div}_x(\nabla_v w) + \frac{h_0^{b2}\alpha}{6\beta^2}\frac{1}{\tau(x)\Theta(x)}\Delta_x w,$$

together with (2.8). In the ballistic regime the ballistic speed is dominant with respect to the thermal speed, and the drift speed is of the order of the ballistic speed, that is, $\alpha \simeq 1$ and $\beta \ll 0$.

Setting, resp., $h_0^b = 0$ and $\tau = 1$, $\Theta = 1$ in (2.15) we obtain the *BS equation for VPFP*:

$$\frac{\partial f}{\partial t} + (v\cdot\nabla_x)f + \frac{1}{2}(\nabla_x\Phi\cdot\nabla_v)f = \frac{1}{2\alpha}\frac{1}{\tau(x)}\mathrm{div}_v(vf + \beta^2\Theta(x)\nabla_v f), \tag{2.16}$$

and the *BS equation for WPFP*:

$$\frac{\partial w}{\partial t} + (v\cdot\nabla_x)w - \frac{1}{2}T_{2\alpha h_0^b}[\Phi]w \tag{2.17}$$

$$= \frac{1}{2\alpha}\mathrm{div}_v(vw + \beta^2\nabla_v w) + \frac{\zeta h_0^b}{6\pi}\mathrm{div}_x(\nabla_v w) + \frac{h_0^{b2}\alpha}{6\beta^2}\Delta_x w,$$

for $\beta \to 0$. Both (2.16) and (2.17) are coupled to the scaled Poisson equation (2.8). Note that in BS the quantum effects are important: neither does the quantum potential term $T_{2\alpha h_0^b}[\Phi]$ become classical, nor does the spatial diffusion operator vanish as $\beta \to 0$.

The ballistic regime is also considered as a high field regime since the effect of the potential dominates the dynamics. We remark that the drift-collision balance regime is an intermediate scaling between the low field scaling and the ballistic one. Further discussions are postponed to the end of Section 5.

3 Low field scaling equations

This section is concerned with formally deriving the drift-diffusion limit of the VPFP and WPFP systems in the LFS as $\eta \to 0$ (see (2.7), (2.8), (2.10)). To this end we set $\eta = \nu$ in (2.5), (2.6) and make a Hilbert expansion of w and Φ in the parameter η :

$$w \simeq w^0 + \eta w^1, \qquad \Phi \simeq \Phi^0 + \eta \Phi^1. \tag{3.1}$$

In lowest order we find that

$$w^0(t,x,v) = \rho(t,x) M_\Theta(v) = \rho(t,x)(2\pi\Theta(x))^{-\frac{N}{2}} \exp\left(-\frac{|v|^2}{2\Theta(x)}\right), \tag{3.2}$$

with $\rho(t,.) = \int w^0(t,.,v)dv \in L^1(\Omega)$. w^1 has to satisfy

$$\begin{aligned} &\frac{1}{\tau(x)} \mathrm{div}_v(vw^1 + \Theta(x)\nabla_v w^1) = g^0 \\ &\quad := (v\cdot\nabla_x)w^0 - T_{\eta h_0}[\Phi^0]w^0 - \frac{\zeta h_0}{6\pi}\frac{1}{\tau(x)\Theta(x)}\mathrm{div}_x(\nabla_v w^0), \end{aligned} \tag{3.3}$$

where Φ^0 satisfies (3.7b) below. Using the Fredholm alternative it is easy to see that the equation

$$\frac{1}{\tau}\mathrm{div}_v(vf + \Theta\nabla_v f) = g,$$

with $g \in L^1(I\!R^N)$ given, has a solution if and only if $\int_{I\!R^N} g dv = 0$.

From (1.9) we easily verify that $T[\Phi]w$ and its classical limit $(-\nabla_x\Phi\cdot\nabla_v w)$ have the same v-moments up to order two. In particular we have

$$\int_{I\!R^N} T[\Phi]w dv = 0, \quad \int_{I\!R^N} vT[\Phi]w dv = \nabla_x\Phi \int_{I\!R^N} w dv. \tag{3.4}$$

Hence $\int_{I\!R^N} g^0(t,x,v)dv = 0 \quad \forall x \in \Omega,\ t \geq 0$, and (3.3) has a unique solution $w^1(t,x,v)$.

Integrating (2.5) (with $\eta = \nu$) in v gives to first order in η :

$$\frac{\partial\rho}{\partial t} + \mathrm{div}_x\left(\int_{I\!R^N} vw^1 dv\right) = \frac{h_0^2}{12}\frac{1}{\tau(x)\Theta(x)}\Delta_x\rho, \tag{3.5}$$

and from (3.3), (3.4) we get

$$\frac{1}{\tau(x)}\int_{\mathbb{R}^N} v w^1 dv = -\int_{\mathbb{R}^N} v g^0 dv = -\nabla_x(\rho\Theta(x)) + \rho\nabla_x\Phi^0 - \frac{\zeta h_0}{6\pi}\frac{1}{\tau(x)\Theta(x)}\nabla_x\rho. \quad (3.6)$$

Our two models, the VPFP and WPFP cases, are obtained from (3.5), (3.6) by resp. setting $h_0 = 0$ and $\tau = 1$, $\Theta = 1$: The LFS limit of the VPFP equation is the standard drift-diffusion system

$$\frac{\partial\rho}{\partial t} + \mathrm{div}_x[\tau(x)\rho\nabla_x\Phi - \tau(x)\nabla_x(\rho\Theta(x))] = 0, \quad (3.7a)$$

$$\mathrm{div}_x(\varepsilon(x)\nabla_x\Phi) = \gamma(\rho - C(x)). \quad (3.7b)$$

The LFS limit of the WPFP equation is also a drift-diffusion equation, where the diffusion constant is increased due to the quantum effects of the QFP-term:

$$\frac{\partial\rho}{\partial t} + \mathrm{div}_x\left[\rho\nabla_x\Phi - \left(1 + \frac{\zeta}{6\pi}h_0 + \frac{h_0^2}{12}\right)\nabla_x\rho\right] = 0, \quad (3.8)$$

coupled to (3.7b).

To finish this section, let us review the boundary conditions for this system. The boundary of the region Ω, which is occupied by the semiconductor device typically consists of two parts: $\partial\Omega = \Gamma_D \cup \Gamma_N$. On the insulating boundaries Γ_N we assume a homogeneous Neumann boundary condition for the electric potential (zero flux) and a reflection operator in the kinetic equation preserving the equilibrium M_Θ. On the Ohmic contacts Γ_D we prescribe the electric potential and the Maxwellian $C(x)M_\Theta$ for the incoming velocities at the boundary. For the corresponding drift-diffusion equations, we consider the following boundary conditions:

$$j \cdot n = 0 \qquad \text{and} \qquad E \cdot n = 0 \quad \text{on} \quad \Gamma_N,$$

where the current j equals the terms in the squared brackets of (3.7a) and (3.8), resp. n denotes a normal vector on $\partial\Omega$. The electric potential Φ is taken constant in space on each connected component of Γ_D, and $\rho(x) = C(x)$. Let us finally remark that a first step in the rigorous proof of this scaling limit has been done recently in [25].

4 Drift-collision balance scaling equations

In Section 2 we derived the *drift-collision balance scaling* (DCBS) for the VPFP and WPFP systems. As we did for the low field scaling, we shall first consider the equation

$$\eta\frac{\partial w}{\partial t} + (v\cdot\nabla_x)w - \frac{\eta}{\nu}T_{\nu h_0}[\Phi]w \quad (4.1)$$
$$= \frac{1}{\nu}\frac{1}{\tau(x)}\mathrm{div}_v(vw + \Theta(x)\nabla_v w) + \frac{\zeta h_0}{6\pi}\mathrm{div}_x(\nabla_v w) + \frac{h_0^2\nu}{12}\Delta_x w,$$

coupled with (2.13). The DCBS for VPFP and WPFP then corresponds to the cases $h_0 = 0$ and $\tau = 1$, $\Theta = 1$, respectively. We recall that $\eta = O(1)$, $\nu \to 0$.

Again, one could proceed as in the previous section by expanding the distribution function and the potential field in terms of ν, and one would obtain a hyperbolic equation for the density. Instead of doing that we apply a Chapman–Enskog expansion that will enable us to obtain higher order correction terms to this hyperbolic equation. In fact we shall find that the diffusion and the quantum correction terms are of order ν in this expansion.

The Chapman-Enskog expansion consists in expanding the distribution function w that solves problem (4.1), (2.13) in power series of ν:

$$w = \sum_{k\geq 0} \nu^k \; w_k, \quad \text{with } \langle w\rangle = \langle w_0\rangle =: \rho \text{ and } \langle w_k\rangle = 0, \; k > 0,$$

and writing $w(x, v, t)$ as a function of ρ and $\nabla_x\Phi$, and their spatial derivatives. Hence, the x– and t–dependence of w only enters through ρ and $\nabla_x\Phi$. Here, $\langle w\rangle$ is the integral of w in velocity variables.

In order to get rid of the time derivative of w in (4.1), we use the mass equation obtained by integrating (4.1) in v,

$$\eta\frac{\partial\rho}{\partial t} + \mathrm{div}_x\langle vw\rangle = \frac{h_0^2\nu}{12}\Delta_x\rho. \tag{4.2}$$

Therefore, we have $w(x, v, t) = w(v; \partial_x^k\rho, \partial_x^j\nabla\Phi)$ with the multi indexes $k = (k_i, \ldots, k_N)$ and $j = (j_1, \ldots, j_N)$, and hence:

$$w_t = \sum_{|k|\geq 0} \frac{\partial w}{\partial\left(\partial_x^k\rho\right)}\; \partial_x^k\rho_t + \sum_{|j|\geq 0} \frac{\partial w}{\partial\left(\partial_x^j\nabla_x\Phi\right)}\; \partial_x^j\,\nabla_x\Phi_t.$$

In order to simplify the notation, we write the previous identity as

$$w_t = D_\rho\, w\cdot\partial_t\rho + D_{\nabla\Phi}w\cdot\partial_t\nabla\Phi. \tag{4.3}$$

Now, we insert (4.1) into (2.13) to get

$$\begin{aligned}\mathrm{div}_x\;(\varepsilon\partial_t\nabla\Phi) = \frac{\gamma}{\eta^N}\,\partial_t\rho &= -\frac{\gamma}{\eta^{N+1}}\,\mathrm{div}_x\langle vw\rangle + \frac{\gamma}{\eta^{N+1}}\,\frac{h_0^2\nu}{12}\Delta_x\rho \\ &= -\frac{\gamma}{\eta^{N+1}}\,\mathrm{div}_x\left(\langle vw\rangle - \frac{h_0^2\nu}{12}\nabla_x\rho\right).\end{aligned} \tag{4.4}$$

Thus, one can find a divergence free vector field $\bar\omega(t, x)$ with

$$\mathrm{rot}_x\frac{1}{\varepsilon}\left(\langle vw\rangle - \frac{h_0^2\nu}{12}\nabla_x\rho\right) = \mathrm{rot}_x\frac{1}{\varepsilon}\bar\omega, \tag{4.5}$$

and then,

$$\varepsilon\partial_t\nabla\Phi = \frac{\gamma}{\eta^{N+1}}\left(-\langle vw\rangle + \frac{h_0^2\nu}{12}\nabla_x\rho + \bar\omega\right). \tag{4.6}$$

Combining (4.3), (4.4) and (4.6) we find

$$\eta w_t = -D_\rho\, w\cdot \mathrm{div}_x \left(\langle vw\rangle - \frac{h_0^2\nu}{12}\nabla_x\rho \right) + \frac{\gamma}{\eta^N}\frac{1}{\varepsilon(x)} D_{\nabla\Phi} w\cdot \left(-\langle vw\rangle + \frac{h_0^2\nu}{12}\nabla_x\rho + \bar\omega \right). \tag{4.7}$$

We remark that the vector field $\bar\omega$ is not uniquely determined by (4.5) and $\mathrm{div}_x\bar\omega = 0$, hence appropriate boundary conditions have to be imposed on $\bar\omega$ at $\partial\Omega$. While it is not yet known how to do this in general, in §6 we shall discuss a way to fix $\bar\omega$ for the a one-dimensional example.

Substituting (4.7) into (4.1) we look for solutions of

$$\begin{aligned} &(v\cdot\nabla_x)w - D_\rho\, w\cdot \mathrm{div}_x \left(\langle vw\rangle - \frac{h_0^2\nu}{12}\nabla_x\rho \right) \\ &+\frac{\gamma}{\eta^N}\frac{1}{\varepsilon(x)} D_{\nabla\Phi} w\cdot \left(-\langle vw\rangle + \frac{h_0^2\nu}{12}\nabla_x\rho + \bar\omega \right) - \frac{\eta}{\nu} T_{\nu h_0}[\Phi]w \\ &= \frac{1}{\nu}\frac{1}{\tau(x)}\mathrm{div}_v(vw + \Theta(x)\nabla_v w) + \frac{\zeta h_0}{6\pi}\mathrm{div}_x(\nabla_v w) + \frac{h_0^2\nu}{12}\Delta_x w. \end{aligned} \tag{4.8}$$

Introducing the expansion in the previous equation and balancing terms of the same order, we shall finally find equations for any order of the approximation. In order to do that we first have to expand the pseudo-differential operator $T_{\nu h_0}[\Phi]w$ in powers of ν,

$$T_{\nu h_0}[\Phi]w = \sum_{k\geq 0} \nu^k\ T^k[\Phi]w,$$

where we assumed sufficient regularity of the potential Φ. From the definition (1.9) one easily sees that the linear differential operators $T^k[\Phi]$ satisfy:

$$T^0[\Phi]w = T_0[\Phi]w = -(\nabla_x\Phi\cdot\nabla_v)w \quad\text{and}\quad T^k[\Phi]w = 0 \text{ for } k \text{ odd}.$$

Generally, $T^k[\Phi]$ (for k even) is a differential operator in v of order $k+1$, involving the $(k+1)$-st derivatives of Φ.

Thus, for the zeroth order approximation, i.e. order ν^{-1} in (4.1), we find

$$\eta(\nabla_x\Phi\cdot\nabla_v)w_0 = \frac{1}{\tau(x)}\mathrm{div}_v(vw_0 + \Theta(x)\nabla_v w_0). \tag{4.9}$$

It is straightforward to check that its solution is given by the drifted Maxwellian

$$w_0(t,x,v) = \rho(t,x)P(t,x,v), \tag{4.10}$$

where

$$P(t,x,v) = (2\pi\Theta(x))^{-N/2}\exp\left(-\frac{|v-U(x)|^2}{2\Theta(x)} \right) \tag{4.11}$$

and $U = \eta\tau\nabla_x\Phi$ is the local drift velocity. Here, the main difference to the standard Chapman-Enskog expansion in rarefied gas dynamics is that the zeroth order approximation depends on space and time variables not only through ρ, but through the electric field as well.

Matching the following orders in ν we find for $k \geq 0$:

$$
\begin{aligned}
(v \cdot \nabla_x) w_k - \sum_{j=0}^{k} \left\{ D_\rho \, w_j \cdot \mathrm{div}_x(\langle v w_{k-j} \rangle) + \frac{\gamma}{\eta^N} \frac{1}{\varepsilon} D_{\nabla \Phi} w_j \cdot (\langle v w_{k-j} \rangle - \bar{\omega}_{k-j}) \right\} \\
+ \frac{h_0^2}{12} D_\rho \, w_{k-1} \cdot \Delta_x \rho + \frac{\gamma}{\eta^N} \frac{1}{\varepsilon} \frac{h_0^2}{12} D_{\nabla \Phi} w_{k-1} \cdot \nabla_x \rho - \eta \sum_{j=0}^{k+1} T^j[\Phi] w_{k+1-j} \\
= \frac{1}{\tau} \mathrm{div}_v (v w_{k+1} + \Theta \nabla_v w_{k+1}) + \frac{\zeta h_0}{6\pi} \mathrm{div}_x (\nabla_v w_k) + \frac{h_0^2}{12} \Delta_x w_{k-1}, \qquad (4.12)
\end{aligned}
$$

where the divergence free fields $\bar{\omega}_{k-j}$ are obtained matching orders of ν in (4.5) for $w = w_{k-j}$. Therefore, the divergence free fields $\bar{\omega}_k$ verify

$$
\begin{aligned}
\mathrm{rot}_x \frac{1}{\varepsilon} \langle v w_k \rangle &= \mathrm{rot}_x \frac{1}{\varepsilon} \bar{\omega}_k, \quad \text{for } k \geq 0, k \neq 1, \qquad (4.13) \\
\mathrm{rot}_x \frac{1}{\varepsilon} \left(\langle v w_1 \rangle - \frac{h_0^2}{12} \nabla_x \rho \right) &= \mathrm{rot}_x \frac{1}{\varepsilon} \bar{\omega}_1, \qquad \text{for } k = 1.
\end{aligned}
$$

Due to the linear structure of the collision operator (i.e. the FP or QFP operator), we find a recursive relationship that defines w_{k+1} in terms of $w_j, j = 0, \ldots, k$ and their moments. As a consequence we also show that the macroscopic equations for the higher order moments

$$
\rho^{(n)} \equiv \langle v^{\otimes n} w \rangle,
$$

are given as a recursive relationship on $\rho_{k+1}^{(n)} \equiv \langle v^{\otimes n} w_{k+1} \rangle$ in terms of $\rho_j^{(m)}$ for $j = 0, \ldots, k$ and $m = 0, \ldots, n+1$.

Here, we are not going to discuss the recursive solvability of the iterative relation (4.12). At the end of this section we will only write down the equation for $n = 1$ and $k = 0$, which yields the order ν–correction to the DCBS equation.

The velocity moments of P, denoted by

$$
m_P^{(n)} \equiv \langle v^{\otimes n} P \rangle,
$$

can be computed recursively from (4.9) by

$$
m_P^{(n)} \;=\; u_\otimes m_P^{(n-1)} + \frac{1}{n} \Theta(x) \Delta_v (m_P^{(n)}). \qquad (4.14)
$$

Here we used the following notation: for any differential operator $\mathcal{L}_v$ (acting on the velocity variable) the abbreviation $\mathcal{L}_v(\rho_k^{(n)})$ shall mean

$$
\mathcal{L}_v(\rho_k^{(n)}) \;=\; \langle \mathcal{L}_v(v^{\otimes n}) w_k \rangle.
$$

Hence, the first four $m_P^{(n)}$ are

$$
\begin{aligned}
m_P^{(0)} &= 1, \\
m_P^{(1)} &= U = \eta \tau \nabla_x \Phi, \qquad (4.15) \\
m_P^{(2)} &= \Theta I + U_\otimes U, \\
m_P^{(3)} &= \Theta I_\otimes U + U_\otimes U_\otimes U,
\end{aligned}
$$

where I is the identity matrix. Taking the $v^{\otimes n}$-moments of the equation (4.12) we find the iterative relation for $\rho_{k+1}^{(n)}, k \geq 0$:

$$\begin{aligned}
&\mathrm{div}_x \rho_k^{(n+1)} - \sum_{j=0}^{k} D_\rho \cdot \rho_j^{(n)} \, \mathrm{div}_x \rho_{k-j}^{(1)} + \frac{\gamma}{\eta^N} \frac{1}{\varepsilon} \sum_{j=0}^{k} D_{\nabla\Phi} \cdot \rho_j^{(n)} \; (-\rho_{k-j}^{(1)} + \bar{\omega}_{k-j}) \\
&+ \frac{h_0^2}{12} D_\rho \cdot \rho_{k-1}^{(n)} \Delta_x \rho + \frac{\gamma}{\eta^N} \frac{1}{\varepsilon} \frac{h_0^2}{12} D_{\nabla\Phi} \rho_{k-1}^{(n)} \cdot \nabla_x \rho - \eta \sum_{j=0}^{k+1} \langle v^{\otimes n} T^j[\Phi] w_{k+1-j} \rangle \\
&= -\frac{n}{\tau} \rho_{k+1}^{(n)} + \frac{\Theta}{\tau} \Delta_v(\rho_{k+1}^{(n)}) - \frac{\zeta h_0}{6\pi} \mathrm{div}_x(\nabla_v(\rho_k^{(n)})) + \frac{h_0^2}{12} \Delta_x(\rho_{k-1}^{(n)}), \quad (4.16)
\end{aligned}$$

where the divergence free fields $\bar{\omega}_{k-j}$ are given by (4.13). Moreover, $\rho_{k+1}^{(0)} = 0$ for any $k \geq 0$, $\rho_0^{(n)} = \rho m_P^{(n)}$ and $\rho_{-1}^{(n)} = 0$ for any $n \geq 0$.

Note that the identity (4.16) is a recursive relation to find $\rho_{k+1}^{(n)}$. In order to do so we have to know the term

$$\eta \sum_{j=0}^{k+1} \langle v^{\otimes n} T^j[\Phi] w_{k+1-j} \rangle. \quad (4.17)$$

In the classical VPFP case this term simply reduces to

$$\frac{n}{\tau} U \otimes \rho_{k+1}^{(n-1)}.$$

In the quantum case one can use the explicit form of the operators $T^j[\Phi]$ to express (4.17) in terms of $\rho_{k+1-j}^{(n-1-j)}$, $j = 0, \ldots, n-1$. However, the higher order terms (in j) give rise to higher order derivatives of the potential Φ, which is non-smooth in typical quantum semiconductor devices (see [20]). Therefore we shall confine ourselves to the first order equation ($k = 0$) and compute the first order approximation of the first moment ($n = 1$). Then we have

$$\begin{aligned}
&\mathrm{div}_x \rho_0^{(2)} - D_\rho \cdot \rho_0^{(1)} \, \mathrm{div}_x \rho_0^{(1)} + \frac{\gamma}{\eta^N} \frac{1}{\varepsilon} D_{\nabla\Phi} \cdot \rho_0^{(1)} \; (-\rho_0^{(1)} + \bar{\omega}_0) - \eta \frac{1}{\tau} U \otimes \rho_1^{(0)} \\
&= -\frac{1}{\tau} \rho_1^{(1)} + \frac{\Theta}{\tau} \Delta_v(\rho_1^{(1)}) - \frac{\zeta h_0}{6\pi} \mathrm{div}_x(\nabla_v(\rho_0^{(1)})).
\end{aligned}$$

Inserting the moments $\rho_0^{(n)}$ from (4.10), (4.15) we finally have

$$\rho_1^{(1)} = \tau \left\{ -\mathrm{div}_x(\Theta \rho I + \rho U \otimes U) + U \mathrm{div}_x(\rho U) - \tau \frac{\gamma}{\eta^{N-1}} \frac{1}{\varepsilon} \rho(-\rho U + \bar{\omega}_0) - \frac{\zeta h_0}{6\pi} \mathrm{div}_x(\rho I) \right\}.$$

Therefore, we have the approximation of order ν of $\rho^{(1)}$ by

$$\rho^{(1)} \simeq \rho_0^{(1)} + \nu \rho_1^{(1)} = j_0 + \nu j_1 \quad (4.18)$$

$$= \rho U + \nu\tau \left\{ -\nabla_x(\Theta\rho) - \rho U \cdot \nabla_x U + \tau \frac{\gamma}{\eta^{N-1}} \frac{1}{\varepsilon} \rho(\rho U - \bar{\omega}_0) - \frac{\zeta h_0}{6\pi} \nabla_x \rho \right\},$$

where $\bar{\omega}_0$ satisfies $\mathrm{div}_x \bar{\omega}_0 = 0$ and

$$\mathrm{rot}_x \frac{1}{\varepsilon}\rho U = \mathrm{rot}_x \frac{1}{\varepsilon}\bar{\omega}_0.$$

Finally, using the continuity equation (4.2) we obtain the DCBS equations

$$\eta \frac{\partial \rho}{\partial t} + \mathrm{div}_x(\rho U + \nu j_1) = \frac{h_0^2 \nu}{12}\Delta_x \rho, \tag{4.19}$$

$$j_1 = \tau \tilde{j}\ ,\ \tilde{j} = -\nabla_x(\Theta\rho) - \rho U \cdot \nabla_x U + \tau \frac{\gamma}{\eta^{N-1}}\frac{1}{\varepsilon}\rho(\rho U - \omega) - \frac{\zeta h_0}{6\pi}\nabla_x \rho, \tag{4.20}$$

$$\mathrm{div}_x \omega = 0 \qquad \text{and} \qquad \mathrm{rot}_x \frac{1}{\varepsilon}\rho U = \mathrm{rot}_x \frac{1}{\varepsilon}\omega, \tag{4.21}$$

$$U = -\eta\tau E, \quad E = -\nabla\Phi \quad \text{and} \quad \mathrm{div}_x(\varepsilon(x)\nabla_x \Phi) = \gamma(\eta^{-N}\rho - C(x)). \tag{4.22}$$

Our two models, the VPFP and WPFP cases, are obtained from (4.19)-(4.22) by resp. setting $h_0 = 0$ and $\tau = 1$, $\Theta = 1$: The DCBS limit of the VPFP equation is the augmented drift-diffusion–Poisson model

$$\eta \frac{\partial \rho}{\partial t} + \mathrm{div}_x(\rho U + \nu j_1) = 0, \tag{4.23}$$

$$j_1 = \tau \tilde{j}\ ,\ \tilde{j} = -\nabla_x(\Theta\rho) - \rho U \cdot \nabla_x U + \tau \frac{\gamma}{\eta^{N-1}}\frac{1}{\varepsilon}\rho(\rho U - \omega), \tag{4.24}$$

$$\mathrm{div}_x \omega = 0 \qquad \text{and} \qquad \mathrm{rot}_x \frac{1}{\varepsilon}\rho U = \mathrm{rot}_x \frac{1}{\varepsilon}\omega, \tag{4.25}$$

$$U = -\eta\tau E, \quad E = -\nabla\Phi \quad \text{and} \quad \mathrm{div}_x(\varepsilon(x)\nabla_x \Phi) = \gamma(\eta^{-N}\rho - C(x)). \tag{4.26}$$

And the DCBS limit of the WPFP equation is also an augmented drift-diffusion–Poisson model, where the diffusion constant is increased due to the quantum effects of the QFP-term:

$$\eta \frac{\partial \rho}{\partial t} + \mathrm{div}_x(\rho U + \nu j_1) = 0, \tag{4.27}$$

$$j_1 = -\left(1 + \frac{\zeta h_0}{6\pi} + \frac{h_0^2}{12}\right)\nabla_x \rho - \rho U \cdot \nabla_x U + \frac{\gamma}{\eta^{N-1}}\frac{1}{\varepsilon}\rho(\rho U - \omega), \tag{4.28}$$

$$\mathrm{div}_x \omega = 0 \qquad \text{and} \qquad \mathrm{rot}_x \frac{1}{\varepsilon}\rho U = \mathrm{rot}_x \frac{1}{\varepsilon}\omega, \tag{4.29}$$

$$U = -\eta\tau E, \quad E = -\nabla\Phi \quad \text{and} \quad \mathrm{div}_x(\varepsilon(x)\nabla_x \Phi) = \gamma(\eta^{-N}\rho - C(x)). \tag{4.30}$$

These are the non-dimensional versions. The dimensionalized equations can be obtained by reversing the scalings in Section 2 and one obtains

$$\frac{\partial \rho}{\partial t} + \mathrm{div}_x(\rho U + \tau \tilde{j}) = 0, \tag{4.31}$$

$$\tilde{j} = -\nabla_x(\Theta\rho) - \rho U \cdot \nabla_x U + \frac{e^2}{m}\frac{\tau}{\varepsilon}\rho(\rho U - \omega), \tag{4.32}$$

$$\mathrm{div}_x \omega = 0 \qquad \text{and} \qquad \mathrm{rot}_x \frac{1}{\varepsilon}\rho U = \mathrm{rot}_x \frac{1}{\varepsilon}\omega, \tag{4.33}$$

$$U = -\frac{e}{m}\tau E, \quad E = -\nabla\Phi \quad \text{and} \quad \mathrm{div}_x(\varepsilon(x)\nabla_x\Phi) = e(\rho - C(x)) \tag{4.34}$$

for the DCBS of the VPFP system, and

$$\frac{\partial \rho}{\partial t} + \mathrm{div}_x(\rho U + \tau \tilde{j}) = 0, \tag{4.35}$$

$$\tilde{j} = -\left(\Theta + \frac{\omega_P \hbar^2}{6\pi m^2 \Theta \tau} + \frac{\hbar^2}{12 m^2 \Theta \tau^2}\right)\nabla_x \rho - \rho U \cdot \nabla_x U + \frac{e^2}{m}\frac{\tau}{\varepsilon}\rho(\rho U - \omega), \tag{4.36}$$

$$\mathrm{div}_x \omega = 0 \qquad \text{and} \qquad \mathrm{rot}_x \frac{1}{\varepsilon}\rho U = \mathrm{rot}_x \frac{1}{\varepsilon}\omega, \tag{4.37}$$

$$U = -\frac{e}{m}\tau E, \quad E = -\nabla\Phi \quad \text{and} \quad \mathrm{div}_x(\varepsilon(x)\nabla_x\Phi) = e(\rho - C(x)) \tag{4.38}$$

for the DCBS of the WPFP system. In the literature, $\mu = \frac{e}{m}\tau$ is referred to as the mobility and is tabulated for different materials and semiconductors geometries. In fact, μ can depend on the local field $E(t,x)$. In this case the above procedure is still valid, yielding the same systems with a field dependent mobility.

Remark 4.1 Our DCBS limit of the VPFP equation (4.23)-(4.26) differs the DCBS limit of the BGK-Boltzmann–Poisson equation that was derived in [11]. The difference appears in the diffusion term: in the VPFP case is isotropic and it is the same as in the (LFS) drift-diffusion equation, i.e. $\nabla_x(\Theta\rho)$, while in the BGK-Boltzmann–Poisson case it is given by $(\Theta + \mu^2 E \otimes E)\nabla_x \rho$. This anisotropy in the diffusion is due to the fact that the leading distribution is not symmetric for the drift–collision balance regime in the BGK-Boltzmann–Poisson system, while the leading term in the expansion w_0 is symmetric with respect to u for the VPFP equation.

The quantum corrected model (4.27)-(4.30) is apparently new. We point out that a related *quantum drift diffusion model* ([21], [22]) has recently been investigated as a simple model for simulating quantum semiconductor devices. That model was derived as a LFS limit ($\eta \ll 1$) from the isothermal quantum hydrodynamic model ([15]) and it differs from our model in the non-linear terms entering in the current (4.28).

Remark 4.2 In both the classical and quantum case one can continue the above process iteratively to find higher ν-order terms in the expansion for $\rho^{(1)}$, the energy $\rho^{(2)}$, or even all higher order moments.

Remark 4.3 As in the case of the BGK-Boltzmann–Poisson system, a new feature in this augmented drift-diffusion system we obtain the field ω in the DCBS equations. Using Maxwell's equations this field can be interpreted as the curl of a magnetic field created by the particles.

5 Ballistic scaling

In Section 2 we presented the *ballistic scaling* (BS) equation for the VPFP system:

$$\frac{\partial f}{\partial t} + (v \cdot \nabla_x) f + \frac{1}{2}(\nabla_x \Phi \cdot \nabla_v) f = \frac{1}{2\alpha} \frac{1}{\tau(x)} \mathrm{div}_v (vf + \beta^2 \Theta(x) \nabla_v f), \tag{5.1}$$

coupled to the scaled Poisson equation (2.8). The ballistic regime appears when $\beta \to 0$ and $\alpha \simeq 1$. Obviously this does not give rise to a macroscopic limit. Formally the limiting equation would be

$$\frac{\partial f}{\partial t} + (v \cdot \nabla_x) f + \frac{1}{2}(\nabla_x \Phi \cdot \nabla_v) f = \frac{1}{2\alpha} \frac{1}{\tau(x)} \mathrm{div}_v (vf). \tag{5.2}$$

Therefore either Hilbert or Chapman–Enskog expansions (along the lines of §3, 4) would not give a drift-diffusion-like system.

Alternatively, one could either study the large time behavior of the macroscopic quantities of (5.1) or introduce a macroscopic closure of (5.1). This approach will be investigated elsewhere.

To illustrate some features of (5.1) let us briefly discuss the large time behavior of the space-homogeneous analogue of (5.1). We consider the operator

$$\mathcal{K} f = \frac{1}{2}(E \cdot \nabla_v) f + \frac{1}{2\alpha} \frac{1}{\tau(x)} \mathrm{div}_v (vf).$$

It is easy to check that any solution with unit mass of the space-homogeneous problem

$$\frac{\partial f}{\partial t} = \mathcal{K} f$$

tends to the equilibrium $f_\infty(v) = \delta(v + \tau E)$ as $t \to 0$, where δ is the Delta distribution. It means that the velocity of the particles concentrate on the drift velocity, which in this scaling is of the order of the ballistic velocity.

However, let us clarify the relation between the BS and the DCBS equations. One can write the non-dimensional parameters η and ν in terms of the parameters α and β obtaining

$$\eta = \frac{\alpha}{\beta}, \quad \nu = 2\alpha\beta. \tag{5.3}$$

Remember that the DCBS is valid when $\eta \simeq 1$ and $\nu \to 0$ which is equivalent to $\alpha \to 0$, $\beta \to 0$ and $\alpha \simeq \beta$. Therefore, the DCBS scaling is an intermediate regime between the LFS and the BS regime when the drift velocity is not high enough.

The BS has been used previously for studying the so-called Child-Langmuir law in semiconductors in the case of the relaxation time operator (see [3] and the references therein). Finally, let us remark that very recently Fokker-Planck type equations have been derived from the Boltzmann equation for semiconductors using the BS and a spherical harmonic expansion (SHE model). In the SHE model one obtains an equation for the distribution function in energy-position space. We refer to [4, 5, 27] for this kind of models.

6 Numerical simulation

The aim of this section is to show that the three presented scaling regimes indeed appear in a realistic simulation of a simple problem. We shall present simulations for a silicon $n^+ - n - n^+$ diode, and we shall see that different regimes (LFS, DCBS, BS) are dominant at different positions $x \in \Omega$ of the device. With this information one can then decompose the domain Ω and use the (locally) relevant model in each subdomain. The main purpose of such a procedure is to restrict the (computationally expensive) original kinetic model to rather small regions, and to solve instead a hybrid model, where the macroscopic limiting equations (drift-diffusion type models) are used wherever possible.

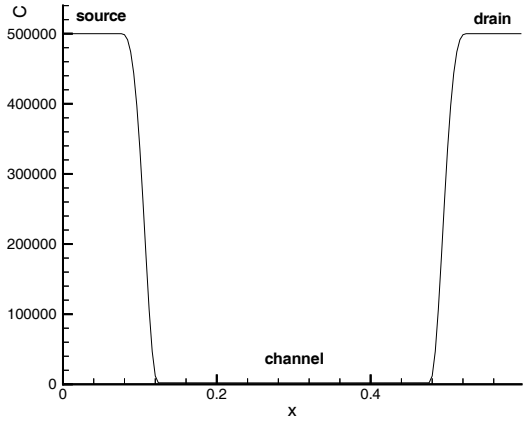

Figure 1: Doping profile of the silicon n^+-n-n^+ device. The applied bias accelerates the electrons from source to drain.

Here, we consider a one dimensional silicon n^+-n-n^+ structure of length $0.6\mu m$ with its doping profile $C(x)$ sketched in Figure 1. The domain of the device is $\Omega = [0, 0.6]$, and the doping profile given by $C(x)$ is a smoothing of the predefined density values $5 \times 10^5/\mu m$ in $0 \leq x \leq 0.1$ and in $0.5 \leq x \leq 0.6$; and $2 \times 10^3/\mu m$ in $0.15 \leq x \leq 0.45$, where we have introduced a smooth intermediate transition with width $0.05\mu m$ close to the junctions. Except for this smoothing of $C(x)$, this is the silicon device analogue of the GaAs device used by Baranger and Wilkins [2]. The numerical outputs between the sharp and smooth $C(x)$ codes have almost any difference and the smoothing of $C(x)$ makes faster and more stable codes.

Our simulations were performed for applied biases V_{bias} from 0V to 2.5V, but to save space we shall only include below the results for $V_{bias} = 2$V. Other parameters: $m = 0.26 \times 0.9109$ $(10^{-30}kg)$, $e = 0.1602$ $(10^{-18}C)$, $k_b = 0.138046 \times 10^{-4}$ $(10^{-18}J/K)$, $\epsilon = 11.7 \times 8.85418$ $(10^{-18}F/\mu m)$, $T = 300K$ and $\mu = 0.0367$. Here, we have chosen constant (in x) lattice temperature and electron mobility, which are resp. given by $\Theta = \frac{k_b}{m}T$ and $\mu = \frac{e}{m}\tau$.

For this device we will now compare the kinetic VPFP model with its scaling limits in the LFS and the DCBS regimes. First we list these three models, together with the boundary conditions that were already presented in §3. The 1D VPFP equation reads

$$f_t + vf_x - \frac{e}{m}E(t,x)f_v = \frac{1}{\tau}(vf + \Theta f_v)_v, \quad 0 < x < 0.6,\ v \in I\!R, \tag{6.1}$$

with the boundary conditions

$$f(t,0,v) \ = \ C(0)\, M_\Theta(v) \ \text{ for } \ v > 0, \tag{6.2a}$$

$$f(t,0.6,v) \ = \ C(0.6)\, M_\Theta(v) \ \text{ for } \ v < 0. \tag{6.2b}$$

The drift-diffusion equation of the LFS regime reads

$$\rho_t + \left(-\mu E(t,x)\rho - \tau\Theta\rho_x\right)_x = 0, \quad 0 < x < 0.6, \tag{6.3}$$

with the boundary conditions

$$\rho(t,0) = C(0), \quad \rho(t,0.6) = C(0.6). \tag{6.4}$$

In 1D the augmented drift-diffusion equation of the DCBS regime reads

$$\rho_t + \left(\rho U - \tau\Theta\rho_x - \tau\rho U U_x + \frac{e^2}{m}\frac{\tau^2}{\varepsilon}\rho(\rho U - \omega)\right)_x = 0, \quad 0 < x < 0.6, \tag{6.5}$$

$$\omega = const, \quad U(t,x) = -\mu E(t,x),$$

with the boundary conditions for the density given by (6.4).

The constant ω is fixed in 1D using the relation (4.4). This equation reads in dimensionalized form

$$\Phi_{txx} = -\frac{e}{\varepsilon}\langle vf\rangle_x.$$

Taking into account that ρU is the first order term in the expansion for the current $j = \langle vf\rangle$ we can fix ω by using (4.6):

$$\omega = (\rho U)|_{x=x_0} + \frac{\varepsilon}{e}\Phi_{tx}|_{x=x_0},$$

where x_0 is an arbitrary point in the region where this augmented drift diffusion model is employed. In general, ω might be time-dependent. However, here we are interested in the steady state and the variation of the potential is negligible in the n^+ regions of the device. Therefore we choose ω to be

$$\omega = -(\mu\rho E)|_{x=x_0}, \tag{6.6}$$

where x_0 is in the right end point of the region where we use the augmented drift-diffusion system.

All three models (6.1), (6.3), (6.5) are coupled to the Poisson equation

$$\Phi_{xx} = \frac{e}{\varepsilon}(\rho(x) - C(x)), \quad 0 < x < 0.6, \tag{6.7}$$

with the boundary conditions $\Phi(t,0) = 0$, $\Phi(t,0.6) = V_{bias}$.

In order to understand the relevant scalings of our problem we will first inspect the local values of the non-dimensional parameters $\eta(x) = \frac{\mu|E(x)|}{\sqrt{\Theta}}$, $\nu = \frac{\tau\sqrt{\Theta}}{L} = const$, $\gamma(x) = \frac{C(x)eL}{\varepsilon_0|E(x)|}$. The values of the field $E(x)$ are here taken from the steady state solution of the VPFP system (6.1), (6.7). Figure 2 (left) shows the local values of η, ν and γ over the whole interval Ω. This way we can monitor in which parts of the device the assumptions of each scaling regime are correct. We realize that $\eta \simeq 1$ and $\nu \simeq 0$ in the channel and, therefore, the DCBS is valid inside the channel region $[0.1, 0.5]$. Also, we see that the LFS is valid in the intervals $[0, x_A]$ and $[x_B, 0.6]$, where x_A is close to 0.1 and x_B is close to 0.5; they will be specified below.

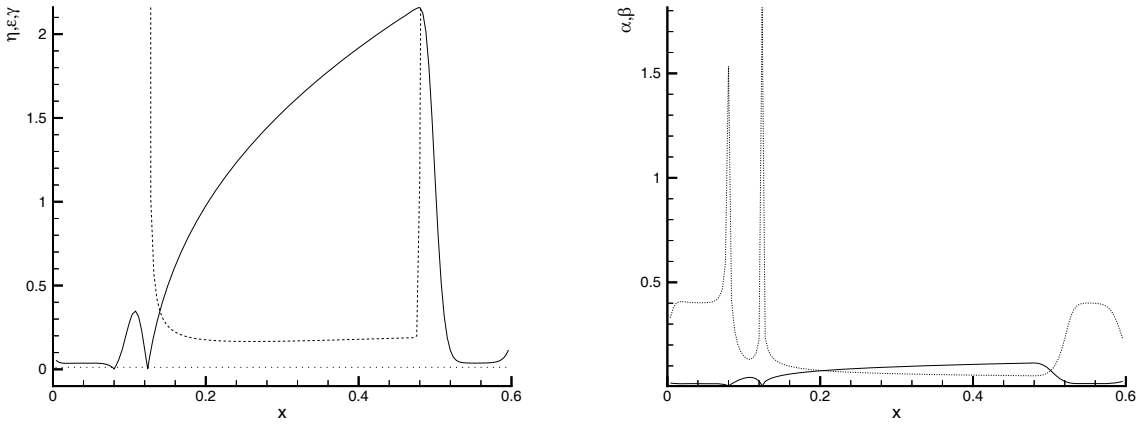

Figure 2: Local non-dimensional parameters, calculated with $E(x)$ from the kinetic simulation results. Left figure: solid line: $\eta(x)$; dashed line: $\nu(x)$; dotted line: $\gamma(x)$. Right figure: solid line: $\alpha(x)$; dotted line: $\beta(x)$.

Let us review this result in terms of the new non-dimensional parameters $\alpha(x)$ and $\beta(x)$ from (5.3). Figure 2 (right) clearly shows that the local values of these parameters satisfy $\alpha \simeq \beta \simeq 0$ in the channel region.

After identifying the dominant scalings in the subregions of the simulation domain Ω we shall now compare the "correct" kinetic reference solution with its drift-diffusion approximations. We shall only compare stationary solutions, i.e. $f_\infty(x,v)$, $\rho_\infty(x)$, which we obtain by using a time marching algorithm for the equations (6.1)-(6.7) until a steady state is reached (the numerical details are deferred to the end of this section).

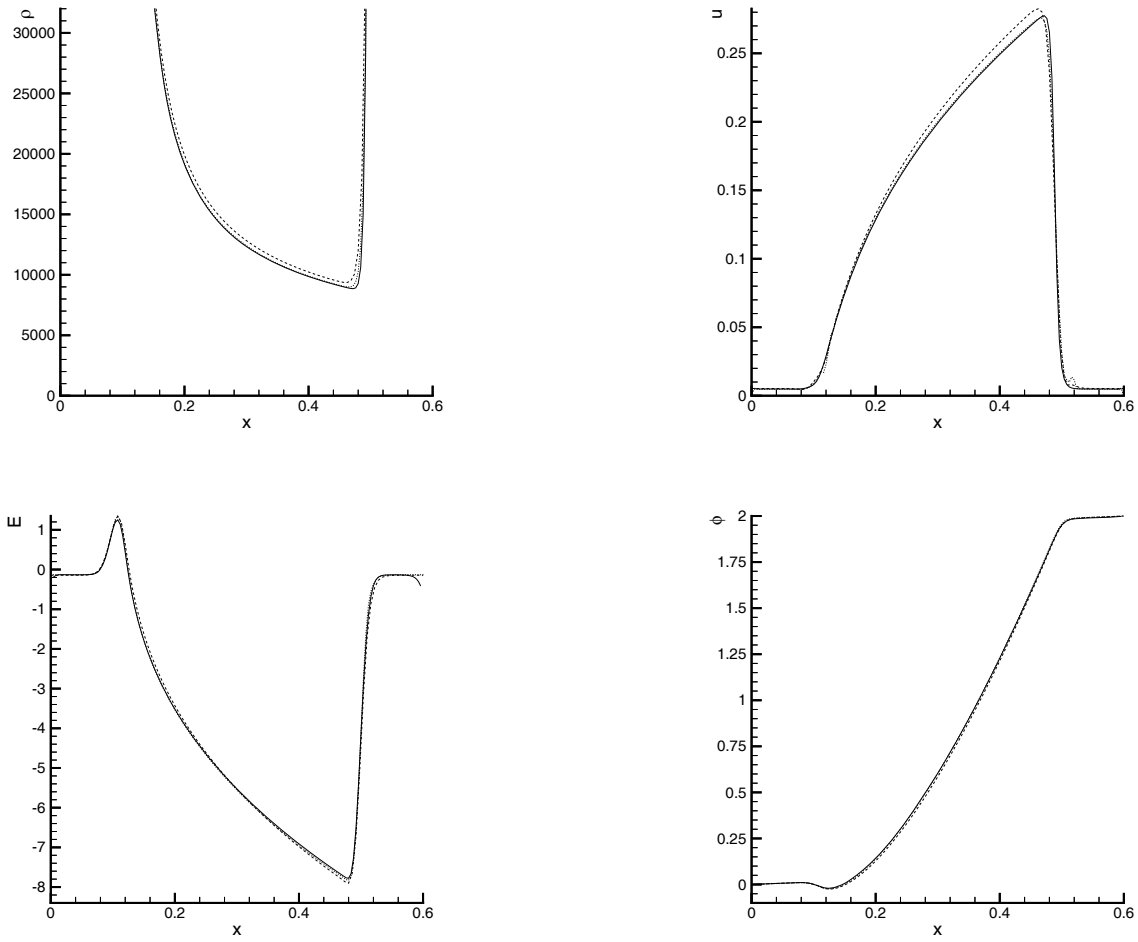

Figure 3: Numerical comparison of kinetic and drift-diffusion models for the silicon n^+-n-n^+ device at $V_{bias} = 2$V. Solid line: the VPFP system; dashed line: the LFS equation; dotted line: the domain decomposition LFS-DCBS-LFS equation. Top left: the charge density ρ in μm^{-1}; top right: the (mean) velocity u in $\mu m/ps$; bottom left: the electric field E in V/μm; bottom right: the potential Φ in V.

In Fig. 3 we first compare the VPFP-solution to the LFS-drift-diffusion model for the whole interval $[0, 0.6]$, and the macroscopic variables are reasonably close.

Next, we make an adaptive domain decomposition and use the LFS model only in $[0, x_A]$ and $[x_B, 0.6]$, and the DCBS in the channel $[x_A, x_B]$, as suggested by Fig. 2. For the hybrid model we match the fluxes from (6.3) and (6.5) at x_A and x_B.

As suggested by the values of α, β, η, ν (see Fig. 2), we choose x_A as the minimum of α inside the channel and x_B as the point where $\eta \simeq \nu \simeq 0$ in the drain (and update x_A and x_B periodically during the time marching algorithm). Here, ω is fixed by the value of ρU at x_B (cf. (6.6)). This produces the results in Figure 3. Compared to the LFS model in the whole device (i.e. the standard drift–diffusion

model), we see a sharp improvement of the charge density $\rho(x)$ and the (mean) velocity $u(x) = \frac{j_\infty}{\rho(x)}$ close to the channel-drain junction; the potential and the field are almost identical to the kinetic results. Here, j_∞ is given by the flux of the drift–diffusion equation equations (6.3) for the LFS model in whole domain, and by the resulting decomposed flux given by the domain decomposition of drift–diffusion and augmented drift–diffusion corresponding to the hybrid LFS-DCBS-LFS model. That means the steady state current j_∞ is given by the local fluxes of the equations (6.3) and (6.5), respectively, according to the decomposed domain.

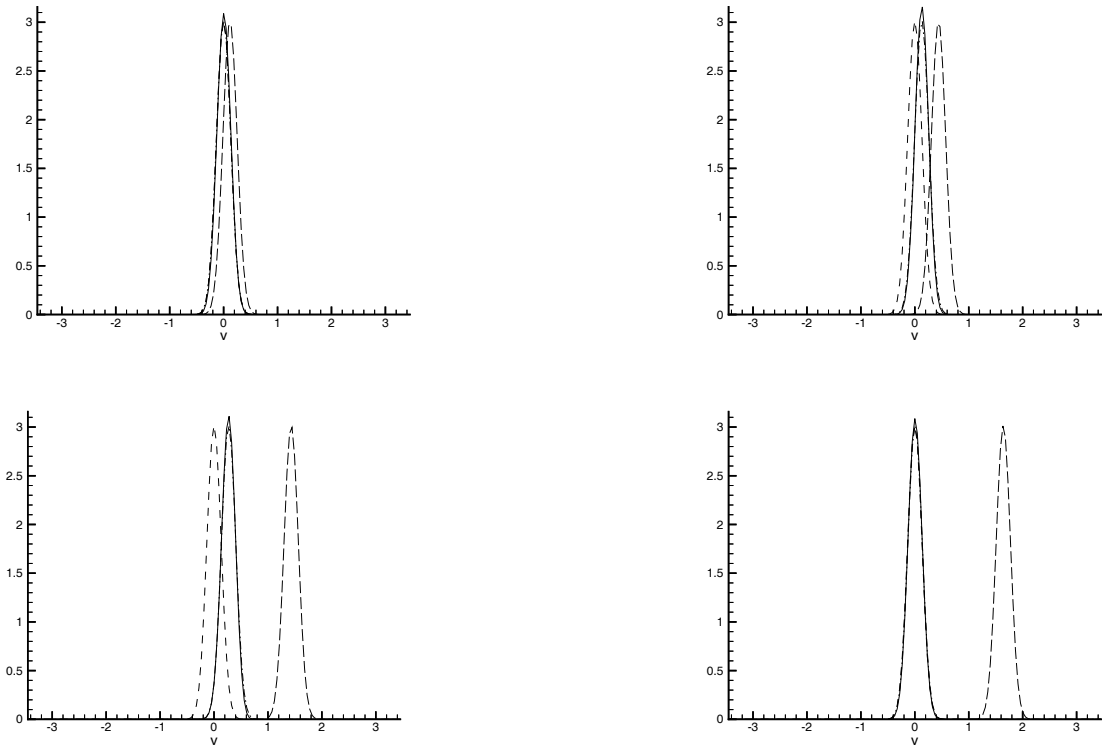

Figure 4: Normalized stationary distribution $f_\infty(x,v)/\rho_\infty(x)$ at several fixed x for $V_{bias} = 2$V, obtained from the kinetic simulation and compared to Maxwellians at lattice temperature Θ, centered at the drift and ballistic velocity. Solid line: kinetic solution; dashed line: $M_\Theta(v)$; dash-dotted line: $M_\Theta(v-U)$; long dashed line: $M_\Theta(v-B)$. Top left: at $x = 0.04\mu m$; top right: at $x = 0.16\mu m$; bottom left: at $x = 0.44\mu m$; bottom right: at $x = 0.56\mu m$.

In Figure 4 we compare the normalized distribution function $f_\infty(x,v)/\rho_\infty(x)$ from the kinetic simulation to its zeroth order approximations in the Hilbert and Chapman-Enskog expansions: $M_\Theta(v)$ for the LFS equation (see (3.2)), $M_\Theta(v-U)$ for the DCBS equation (see (4.10), (4.11)) and $M_\Theta(v-B)$ for the BS equation. Here, the drift velocity $U(x)$ is $-\mu E(x)$ and the ballistic velocity $B(x)$ is $\sqrt{\frac{2e}{m}\Phi(x)}$.

This formula for $B(x)$ follows from (2.1) together with the fact that the electrons are injected at the source with zero mean velocity (see (6.2a)), and since we calibrated the potential by $\Phi(0) = 0$. The "ballistic Maxwellian" is just a way to visualize the ballistic velocity compared to the others. Here, the values of E and Φ are taken from the kinetic simulation, but this point is not important since the values of E and Φ agree very well between the kinetic results and the hybrid LFS-DCBS-LFS results.

Finally, we show in Figure 5 the current-voltage (ρ_∞, V_{bias}) curves for this device given by the kinetic simulation, the LFS model (standard drift-diffusion system), and the hybrid LFS-DCBS-LFS models (drift-diffusion/augmented drift-diffusion domain decomposition), for applied biases in the interval $0 - 2.5$V. The curve given by the hybrid LFS-DCBS-LFS domain decomposition yields the best approximation to the kinetic curve for applied voltages greater than 0.4V. One has to keep in mind that the LFS is the dominant regime for small voltages and hence for low fields. This is the reason why the results of the LFS-DCBS-LFS are not good for small applied voltages.

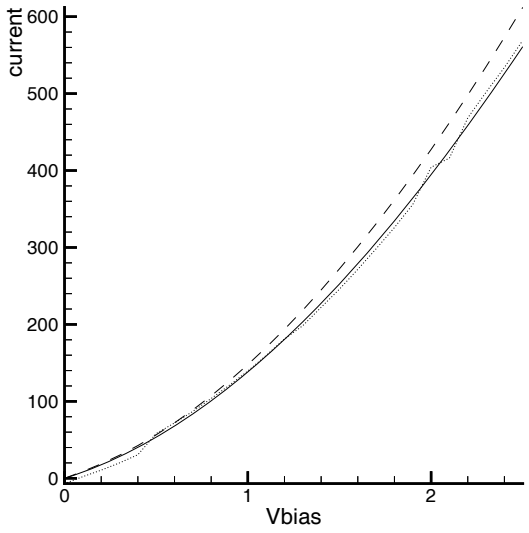

Figure 5: Current-voltage characteristics for the silicon n^+-n-n^+ device. Solid line: the VPFP system; dashed line: the LFS system (drift–diffusion) in the whole device; dotted line: hybrid LFS–DCBS–LFS system.

The last figures of this section are devoted to the ballistic scaling. For illustration purposes we increase the value of the mobility by about a factor of 10 to $\mu = 0.3$. This change is not arbitrary; in fact, the key difference between the set of parameters for a silicon device and the important GaAs parameter set is the higher mobility in the latter case. For the sake of simplicity we have not included here the results for the GaAs device, but we show that the ballistic regime is the

dominant regime in the channel for the standard GaAs parameter set. In Figure 6 we plot the non-dimensional local parameters $\alpha(x)$ and $\beta(x)$, and we realize that the dominant scaling in the channel is now the BS, since $\alpha \simeq 1$ and $\beta \simeq 0$.

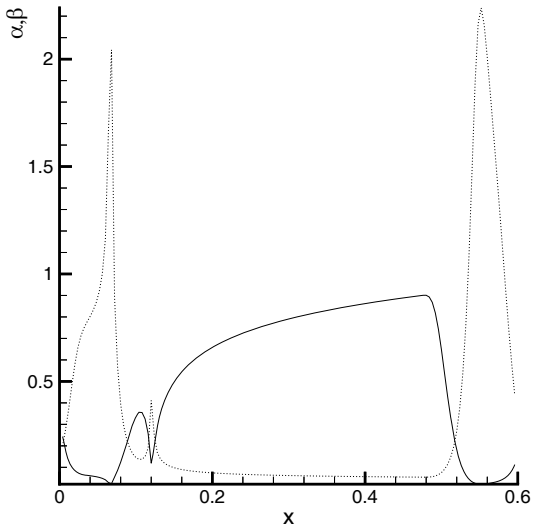

Figure 6: Local non-dimensional parameters, calculated with $E(x)$ from the kinetic simulation results for higher mobility. Solid line: $\alpha(x)$; dotted line: $\beta(x)$.

In Figure 7 we plot the normalized distribution functions for the same applied potential $V_{bias} = 2$V, and we observe that the "ballistic Maxwellian" gives the closest match (with respect to the mean velocity) to the kinetic solution in the channel. The first order approximations of both the LFS and the DCBS are far from the real (kinetic) solution in the channel.

Finally, we shall illustrate even more clearly that the "real regime" in the channel region is now the BS. To this end we solve the reduced VPFP system with $\beta = 0$ (i.e. we set $\Theta = 0$ in (6.1)) and compare the results with the original VPFP results at the level of normalized distribution functions in steady state. In Figure 8 we only plot this distribution function at one point x in the channel region, and we see that it is a good approximation for the solution of the full VPFP system in this case.

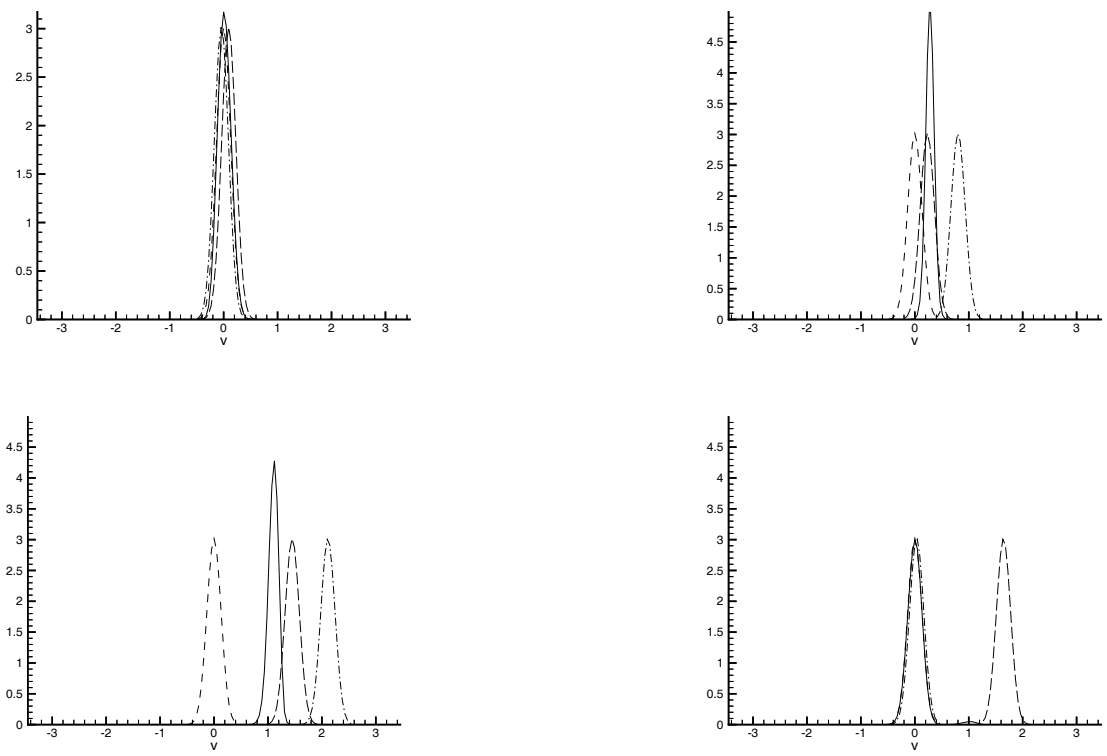

Figure 7: Normalized stationary distribution $f_\infty(x,v)/\rho_\infty(x)$ at several fixed x for $V_{bias} = 2$V and higher mobility, obtained from the kinetic simulation and compared to Maxwellians at lattice temperature Θ, centered at the drift and ballistic velocity. Solid line: kinetic solution; dashed line: $M_\Theta(v)$; dash-dotted line: $M_\Theta(v-U)$; long dashed line: $M_\Theta(v-B)$. Top left: at $x = 0.04\mu m$; top right: at $x = 0.16\mu m$; bottom left: at $x = 0.44\mu m$; bottom right: at $x = 0.56\mu m$.

6.1 Numerical details

For the discretization of the kinetic VPFP system (6.1), (6.7) we use a uniform grid both in x and in v, with 150×150 points. We cut the velocity space at $v = -a$ and $v = a$ and impose homogeneous Neumann boundary conditions there (extrapolation of the numerical solution from inside the domain to the boundary). Our simulations showed that $a = 3.5\mu m/ps$ is large enough. For the LFS equation (6.3) and the DCBS equation (6.5) we also use a uniform grid in x with 150 points for the interval $[0, 0.6]$.

In our simulations we use the WENO (i.e. weighted ENO) scheme developed in [17]. ENO (developed in [28]) and WENO schemes are designed for hyperbolic conservation laws or other problems containing either discontinuous solutions or solutions with sharp gradients. The algorithms are very stable in all the numerical

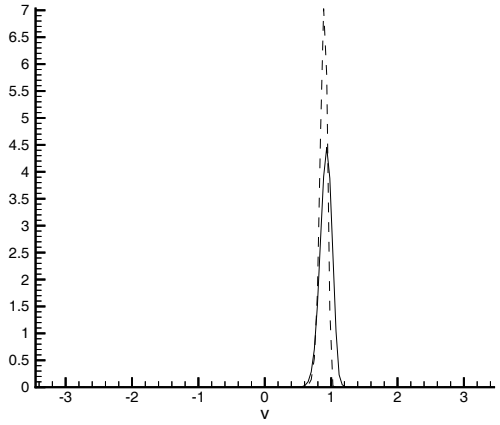

Figure 8: Kinetic simulation results at $V_{bias} = 2$V for the normalized stationary distribution $f_\infty(x,v)/\rho_\infty(x)$ in the channel at $x = 0.32\mu m$ for higher mobility. Solid line: VPFP system; dashed line: reduced VPFP system with $\beta = 0$.

simulations. The FP collision operator and the diffusion terms in the LFS and the DCBS equations are considered sources of the conservation law and approximated by finite differences. For the time integration of the kinetic and the drift-diffusion equations we use a Runge-Kutta method and we update the self-consistent potential Φ at each time step by solving the Poisson equation (6.7). This iterative time stepping is repeated until a steady state (f_∞ or ρ_∞) is reached.

Let us remark that the main aim of a domain decomposition technique using scaling limit models, as sketched in this section, is to save computational time. Our simulations were carried out on a Pentium II 400 MHz and the computational time for kinetic runs is about 35 minutes, compared to 30 seconds for a hybrid LFS-DCBS-LFS domain-decomposition run.

Acknowledgments

Partially supported by the grants ERBFMRXCT970157 (TMR-Network) from the EU, the bilateral DAAD-NSF Program (315/PPP/ru-ab), the DFG under Grant-No. MA 1662/1-2 and DGES (Spain) PB95-1203. The authors are grateful to the hospitality and financial support of the ESI, Vienna and TICAM, Austin, where part of this research was carried out. The second author was supported by the DGESIC MEC-Spain Perfeccionamiento de Doctores en el Extranjero fellowship. The third author is supported by the NSF DMS 9623037. The fourth author is supported by the NSF ECS-9627849 and by the Army Research Office under grant DAAG55-97-1-0318.

References

[1] A. Arnold, J.L. López, P.A. Markowich, J. Soler, *An Analysis of Quantum Fokker–Planck Models: A Wigner Function Approach*, preprint TMR.

[2] H.U. Baranger, J.W. Wilkins, *Ballistic structure in the electron distribution function of small semiconducting structures: General features and specific trends* , Physical Review B, **36**, 1487–1502, 1987.

[3] N. Ben Abdallah, P. Degond, *The Child-Langmuir law for the Boltzmann equation of semiconductors*, SIAM J. Math. Anal., **26**, 364–398, 1995.

[4] N. Ben Abdallah, P. Degond, *On a hierarchy of macroscopic models for semiconductors*, J. Math. Phys., **37**, 3306–3333, 1996.

[5] N. Ben Abdallah, P. Degond, P. Markowich, C. Schmeiser, *High Field Approximations of the Spherical Harmonics Expansion Model for Semiconductors*, preprint TMR.

[6] A.O. Caldeira, A.J. Leggett, *Path Integral Approach to Quantum Brownian Motion*, Physica A, **121**, 587–616, 1983.

[7] J.A. Carrillo, G. Toscani, *Exponential convergence toward equilibrium for homogeneous Fokker-Planck-type equations*, Math. Meth. Appl. Sci., **21**, 1269–1286, 1998.

[8] C. Cercignani, I.M. Gamba, J.W. Jerome and C.W. Shu, *Device Benchmark Comparisons via Kinetic, Hydrodynamic, and High-Field Models*, to appear in Computer Methods in Applied Mechanics and Engineering, 1999.

[9] C. Cercignani, I.M. Gamba, J. W. Jerome, C. Shu, *A Domain Decomposition Method for Silicon Devices*, to appear in Transp. Theory Stat. Phys.

[10] C. Cercignani, I.M. Gamba, C.L. Levermore, *A High Field Approximation to a Boltzmann–Poisson System in Bounded Domains*, Applied Math Letters, **4**, 111–118, 1997.

[11] C. Cercignani, I.M. Gamba, C.D. Levermore, *A High field Approximation to a Boltzmann-Poisson System in Bounded Domains*, preprint 1998.

[12] C. Cercignani, R. Illner, M. Pulvirenti, *The Mathematical Theory of Diluted Gases*, Springer–Verlag, 1994.

[13] L. Diósi, *Caldeira-Leggett master equation and medium temperatures*, Physica A, **199**, 517–526, 1993.

[14] D.K. Ferry, R.O. Grondin, *Physics of submicron devices*, Plenum Press, New York, 1991.

[15] C.L. Gardner, *The quantum hydrodynamic model for semiconductor devices*, SIAM J. Appl. Math., **54** (2), 409–427, 1994.

[16] H.L. Grubin, T.R. Govindan, J.P. Kreskovsky, M.A. Stroscio, *Transport via the Liouville Equation and Moments of Quantum Distribution Functions*, Solid State Electr., **36**, 1697–1709, 1993.

[17] G. Jiang, C.-W. Shu, *Efficient implementation of weighted ENO schemes*, J. Comput. Phys., **126**, 202–228, 1996.

[18] N. Kluksdahl, A.M. Kriman, D.K. Ferry, C. Ringhofer, *Self-consistent study of the resonant tunneling diode*, Phys. Rev. B., **39**, 7720–7735, 1989.

[19] S. Kogan, *Electronic noise and fluctuations in solids*, Cambridge University Press, 1996.

[20] P.A. Markowich, C.A. Ringhofer, C. Schmeiser, *Semiconductor Equations*, Springer, New York, 1990.

[21] R. Pinnau, *The Linearized Transient Quantum Drift Diffusion Model - Stability of Stationary States*, to appear in Z. angew. Math. Mech., 1999.

[22] R. Pinnau, A. Unterreiter, *The Stationary Current–Voltage Characteristics of the Quantum Drift Diffusion Model*, to appear in SIAM J. Numer. Anal., 1999.

[23] F. Poupaud, *Runaway Phenomena and Fluid Approximation Under High Fields in Semiconductor Kinetic Theory*, Z. Angew. Math. Mech., **72**, 359–372, 1992.

[24] F. Poupaud, *Derivation of a hydrodynamic systems hierarchy from the Boltzmann equation*, Appl. Math. Lett., **4**, 75–79, 1991.

[25] F. Poupaud, J. Soler, *Parabolic limit and stability of the Vlasov-Poisson-Fokker-Planck system*, preprint TMR.

[26] L. Reggiani, *Hot–Electron Transport in Semiconductors*, Topics in Applied Physics, Springer–Verlag, New York, 1985.

[27] C., Schmeiser, A. Zwirchmayr, *Elastic and drift-diffusion limits of electron-phonon interaction in semiconductors*, Math. Models Methods Appl. Sci., **8**, 37–53, 1998.

[28] C.-W. Shu, S. Osher, *Efficient implementation of essentially non-oscillatory shock capturing schemes II*, J. Comput. Phys., **83**, 32–78, 1989.

[29] P.C. Stichel, D. Strothmann, *Asymptotic analysis of the high field semiconductor Boltzmann equation*, Physica A, **202**, 553–576, 1994.

[30] M.A. Stroscio, *Moment-Equation Representation of the Dissipative Quantum Liouville Equation*, Superlattices and Microstructures, **2**, 83–87, 1986.

[31] C. M. van Vliet, *Macroscopic and Microscopic Methods for noise in Devices*, IEEE Transactions on electron devices, **41**, 1902-1915, 1994.

[32] E. Wigner, *On the quantum correction for thermodynamic equilibrium*, Phys. Rev., **40**, 749–759, 1932.